

# Future species composition will affect forest water use after loss of eastern hemlock from southern Appalachian forests

STEVEN BRANTLEY,<sup>1,2,3</sup> CHELCY R. FORD,<sup>2</sup> AND JAMES M. VOSE<sup>2,4</sup>

<sup>1</sup>Department of Forest Resources, University of Minnesota, St. Paul, Minnesota 55108 USA

<sup>2</sup>USDA Forest Service, Southern Research Station, Coweeta Hydrologic Lab, Otto, North Carolina 28763 USA

**Abstract.** Infestation of eastern hemlock (*Tsuga canadensis* (L.) Carr.) with hemlock woolly adelgid (HWA, *Adelges tsugae*) has caused widespread mortality of this key canopy species throughout much of the southern Appalachian Mountains in the past decade. Because eastern hemlock is heavily concentrated in riparian habitats, maintains a dense canopy, and has an evergreen leaf habit, its loss is expected to have a major impact on forest processes, including transpiration ( $E_t$ ). Our goal was to estimate changes in stand-level  $E_t$  since HWA infestation, and predict future effects of forest regeneration on forest  $E_t$  in declining eastern hemlock stands where hemlock represented 50–60% of forest basal area. We used a combination of community surveys, sap flux measurements, and empirical models relating sap flux-scaled leaf-level transpiration ( $E_L$ ) to climate to estimate the change in  $E_t$  after hemlock mortality and forecast how forest  $E_t$  will change in the future in response to eastern hemlock loss.

From 2004 to 2011, eastern hemlock mortality reduced annual forest  $E_t$  by 22% and reduced winter  $E_t$  by 74%. As hemlock mortality increased, growth of deciduous tree species—especially sweet birch (*Betula lenta* L.), red maple (*Acer rubrum* L.), yellow poplar (*Liriodendron tulipifera* L.), and the evergreen understory shrub rosebay rhododendron (*Rhododendron maximum* L.)—also increased, and these species will probably dominate post-hemlock riparian forests. All of these species have higher daytime  $E_L$  rates than hemlock, and replacement of hemlock with species that have less conservative transpiration rates will result in rapid recovery of annual stand  $E_t$ . Further, we predict that annual stand  $E_t$  will eventually surpass  $E_t$  levels observed before hemlock was infested with HWA. This long-term increase in forest  $E_t$  may eventually reduce stream discharge, especially during the growing season. However, the dominance of deciduous species in the canopy will result in a permanent reduction in winter  $E_t$  and possible increase in winter stream discharge. The effects of hemlock die-off and replacement with deciduous species will have a significant impact on the hydrologic flux of forest transpiration, especially in winter. These results highlight the impact that invasive species can have on landscape-level ecosystem fluxes.

**Key words:** *Adelges tsugae*; *Betula lenta*; eastern hemlock; evapotranspiration; hemlock woolly adelgid; invasive species; Jarvis model; *Rhododendron maximum*; sap flux; *Tsuga canadensis*; vapor pressure deficit; water use.

## INTRODUCTION

Accurately quantifying changes in ecosystem function (e.g., productivity, hydrology, and so forth) following introduction of an invasive species is a challenging but important step in providing guidance to prioritizing mitigation and restoration strategies. This is especially true where landscape-level processes, such as the balance between forest evapotranspiration (ET) and runoff, affect adjacent ecosystems such as streams, and ecosys-

tem services such as freshwater supply. Invasive plant species have been documented to directly or indirectly alter the hydrologic cycle in a wide range of ecosystems. For example, in Florida, the nonnative invasive *Melaleuca quinquenervia* (tea tree) increases ET rates and decreases water table depth (Gordon 1998). In the western United States, encroachment of velvet mesquite (*Prosopis velutina*) into riparian areas increases ET, causes growing-season ET to exceed precipitation input, and decreases groundwater table depth (Scott et al. 2006). Similarly, salt cedar (*Tamarix ramosissima*) invasion into riparian stands decreases transpiration and productivity of native Fremont cottonwood stands in the western United States (Pataki et al. 2005).

Tree die-off from insect infestation is one of the most important direct effects of invasive species on ecosystem function, and affects ecohydrological processes through reduction in canopy cover (Adams et al. 2012). Invasive insects, such as the hemlock woolly adelgid (HWA,

Manuscript received 16 April 2012; revised 4 October 2012; accepted 3 January 2013. Corresponding Editor: J. A. Jones.

<sup>3</sup> Present address: Coweeta Hydrologic Lab, 3160 Coweeta Lab Rd., Otto, North Carolina 28763 USA.

E-mail: sbrantle@umn.edu

<sup>4</sup> Present address: USDA Forest Service, Southern Research Station, Center for Integrated Forest Science and Synthesis (CIFSS), North Carolina State University, Raleigh, North Carolina 27695 USA.

*Adelges tsugae* Annand), that change community composition through extirpation of foundation species (Ellison et al. 2005, Spaulding and Rieske 2010, Krapfl et al. 2011), are likely to have a lasting effect on hydrologic function of forests. Recent work in eastern North American forests is beginning to estimate the functional changes resulting from the loss of eastern hemlock, *Tsuga canadensis* (L.) Carr. (Pinaceae), after infestation with HWA (Ellison et al. 2005, Daley et al. 2007, Ford and Vose 2007, Nuckolls et al. 2009, Krapfl et al. 2011). In the southern Appalachians, transpiration is a large component ( $\geq 50\%$ ) of the hydrologic budget (Vose and Swank 1994), and loss of a foundation species, especially an evergreen species such as eastern hemlock that transpires and intercepts water year-round, is likely to affect forest ET. In the short term, eastern hemlock loss is projected to cause a significant decline in annual stand transpiration (10%) and an even greater decline in winter transpiration (30%) (Ford and Vose 2007), but long-term effects will vary with community trajectory (Spaulding and Rieske 2010, Ford et al. 2012). Currently there is a need to predict how forest  $E_t$  will respond to future community composition.

Long-term changes in forest ET due to hemlock loss will depend on future species composition, specifically the composition of tree species and the presence or absence of *Rhododendron maximum* L. (Ericaceae), a large, evergreen understory woody shrub. Recent research on vegetation dynamics in eastern hemlock stands undergoing simulated and actual mortality from HWA shows that regeneration in these communities is dominated by rhododendron where this shrub is already present (Elliott and Vose 2010, Krapfl et al. 2011, Ford et al. 2012). Rhododendron forms dense understory thickets that alter soil nutrient availability and confer low rates of successful seedling establishment and growth in the understory (Clinton and Vose 1996, Wurzbarger and Hendrick 2007). In areas where rhododendron is absent, studies suggest that a mix of *Acer*, *Betula*, *Fagus*, and *Quercus* canopy genera, if they can become established, will most likely replace declining hemlock (Orwig and Foster 1998, Spaulding and Rieske 2010, Ford et al. 2012). Two species are of particular interest: red maple *Acer rubrum* L. (Aceraceae) and sweet birch *Betula lenta* L. (Betulaceae). Red maple is ubiquitous throughout low-elevation southern Appalachian forests, and has been increasing in importance (Elliott et al. 1999), particularly in response to disturbance (Elliott and Swank 2008, Elliott and Vose 2010). Sweet birch, also a large component of the mesic hemlock cove community type, is an early-successional species, has increased in importance in mesic hemlock cove areas following disturbance (Elliott et al. 1999, Elliott and Swank 2008), and dominates forest dynamics following hemlock mortality in northeastern forests (Orwig and Foster 1998, Eschtruth et al. 2006, Daley et al. 2007).

Our goals were to estimate recent changes in stand-level transpiration ( $E_t$ ) after HWA infestation and to predict future changes in stand  $E_t$  as eastern hemlock is replaced. We used a combination of direct measurements of community change, sap flux density and climate, and modeled potential recovery of  $E_t$  under projected changes in community composition through 2050. We hypothesized that deciduous species likely to replace hemlock would have a less conservative instantaneous  $E_L$ , and therefore higher  $E_t$ , than hemlock; however, rhododendron  $E_L$  would be more comparable to hemlock  $E_L$ . We then explored how phenological differences between replacement species and hemlock would affect seasonal patterns of  $E_t$ . We focused particularly on autumn and winter  $E_t$ , with the goal of simulating how seasonal patterns of forest  $E_t$  might be altered permanently due to differences in phenology, but recognizing that rhododendron might compensate partially for hemlock loss.

## METHODS

### Study site

This study was conducted at the USDA Forest Service Coweeta Hydrologic Laboratory. The Coweeta basin is a  $\sim 5400$ -ha watershed located in Macon County, North Carolina, USA, and is part of the Nantahala Mountain Range. Climate in the basin is classified as marine, humid temperate (Swift et al. 1988). Average annual precipitation on the valley floor is 1794 mm. Mean annual temperature is  $12.6^\circ\text{C}$ , but has been increasing at a rate of  $0.5^\circ\text{C}$  per decade since the late 1970s to early 1980s (Laseter et al. 2012).

Measurement of sap flux density took place on two study plots, each  $400\text{ m}^2$  in area, which were located in the riparian corridor ( $\sim 700\text{ m}$  above sea level) along Shope Fork, a third-order stream draining the northern section of the Coweeta basin. Species composition in study plots was dominated by eastern hemlock ( $\sim 50\%$  of the basal area); rosebay rhododendron ( $\sim 2000$  stems/ha and  $\sim 5\%$  basal area); and sweet birch ( $\sim 5\%$  basal area) (Brown 2004). The remaining 40% of basal area was composed of various hardwood species, including red maple as well as *Liriodendron tulipifera* L. (Magnoliaceae), *Nyssa sylvatica* Marsh. (Cornaceae), *Quercus* spp., and *Carya* spp.

Estimates of stand  $E_t$  were based on community data from four separate intensive hemlock study plots, each  $400\text{ m}^2$  in area, located in riparian corridors along Shope Fork and Ball Creek. In 2004, species composition in these plots was dominated by eastern hemlock (61% of the basal area), rosebay rhododendron (9% basal area), and sweet birch (7% basal area). The remaining 23% of basal area was composed primarily of the various hardwood species previously listed, including red maple. Although other evergreens were present, i.e., *Kalmia latifolia* L. (Ericaceae) and *Pinus strobus* L. (Pinaceae), occurrence of these species was not consistent across plots and together they represented  $<2\%$  of total basal

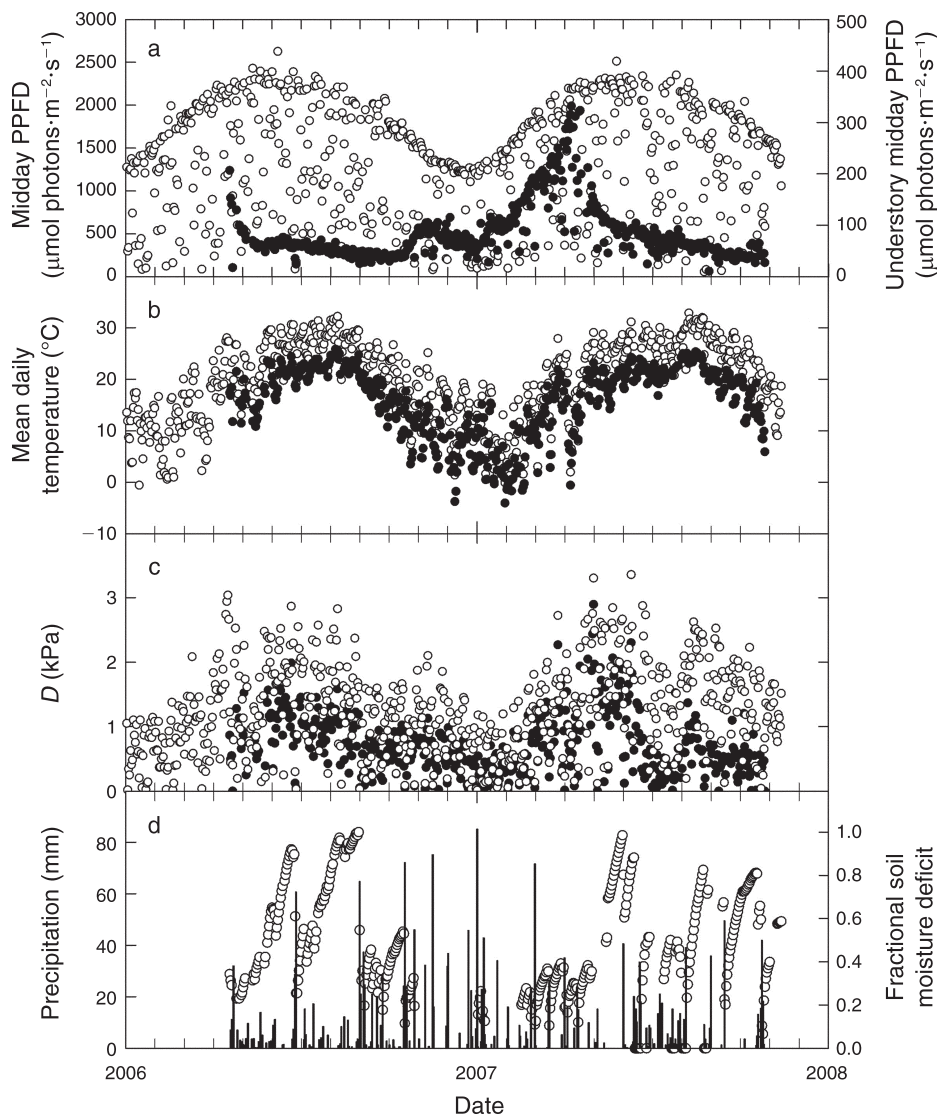


FIG. 1. (a) Photosynthetic photon flux density (PPFD), (b) air temperature, and (c) vapor pressure deficit ( $D$ ) for hemlock study sites (solid circles; below canopy,  $\sim 9$  m above ground surface) and from a nearby ( $\sim 1$  km) open-field meteorological station (open circles). (d) Daily precipitation (vertical bars) and soil moisture deficit, an index of relative soil moisture (open circles). Data from April 2006–November 2007 are shown.

area. Mean leaf area index (LAI) among plots was  $8.0 \pm 0.9$  m<sup>2</sup>/m<sup>2</sup>, 55% of which was eastern hemlock, and 78% of which was eastern hemlock, rhododendron, red maple, and sweet birch.

#### *Climate data*

An open-field climate station (CS01), located  $\sim 1$  km from the site, measured the following variables every 1 min and logged 15- and 60-min averages: air temperature ( $T$ ), relative humidity (RH; model HMP45C, Campbell Scientific, Logan, Utah, USA), rainfall, and solar radiation (W/m<sup>2</sup>, 8–48, Epply Lab, Newport, Rhode Island, USA) (Fig. 1). From ambient  $T$ , saturation vapor pressure ( $e_s$ ) was calculated according to Lowe (1977). Actual vapor pressure ( $e_a$ ) was

calculated from fractional RH and  $e_s$ . Air vapor pressure deficit ( $D$ ) was calculated as the difference between  $e_s$  and  $e_a$ . Photosynthetic photon flux density (PPFD;  $\mu\text{mol photons}\cdot\text{m}^{-2}\cdot\text{s}^{-1}$ ) incident on the upper canopy was estimated from solar radiation measurements by assuming that 50% was in the 400–700 nm wavelength (Landsberg and Waring 1997) and a conversion factor of 4.608  $\mu\text{mol quanta/J}$  (Campbell and Norman 1998).

Climate variables were also measured within the two sap flux plots at a height of 9 m above the forest floor ( $\sim 2$  m above the rhododendron shrub canopy) (Fig. 1). Six GaAsP photodiodes (Model G1118, Hamamatsu, Bridgewater, New Jersey, USA; Pontauiller 1990) calibrated against a commercial quantum sensor (LI190, LI-

COR, Lincoln, Nebraska, USA) were mounted in two arrays on top of two towers to represent PPFD below the canopy (i.e., incident on the rhododendron canopy). One RH and  $T$  sensor (model HMP45C; Campbell Scientific, Logan, Utah, USA) was mounted just below one of the PPFD arrays. Sensors were queried every 30 s and 15-min averages were logged. Soil moisture at 0–30 cm depth was estimated at two locations using time domain reflectometry (TDR, model CS616, Campbell Scientific, Logan, Utah, USA). Due to the high organic matter content in these soils, we developed calibration curves relating sensor period output to volumetric water content ( $\theta$ ) on a soil sample taken from the plot. Volumetric water content was converted to soil moisture deficit (SMD) according to Granier and Loustau (1994), using the following equation:

$$\text{SMD} = \frac{\theta_{\max} - \theta}{\theta_{\max} - \theta_{\min}} \quad (1)$$

where  $\theta_{\max}$  and  $\theta_{\min}$  are the highest and lowest observed values, respectively, over the entire sampling period.

#### *Sap flux density measurements*

In the two sap flux plots, we installed constant heat thermal dissipation sensors (Granier 1985) to determine sap flux density ( $J_s$ ;  $\text{g H}_2\text{O} \cdot \text{m}^{-2} \text{ sapwood} \cdot \text{s}^{-1}$ ) of the outer 2 or 3 cm of the active xylem of four species: eastern hemlock, sweet birch, red maple, and rhododendron. We monitored  $J_s$  in 16 *T. canadensis* trees during 2004–2005, prior to HWA infestation. Sap flux density in seven sweet birch trees, three red maple trees, and six rhododendron shrubs was monitored from April 2006 to October 2008. Sample trees and shrubs with stem diameters measuring  $\leq 45$  cm dbh at 1.37 m (trees) or 1.1–1.3 m (shrubs) above the ground surface had 2-cm probes installed, whereas those with dbh  $> 45$  cm had 3-cm probes installed. Based on increment cores taken from adjacent *T. canadensis* trees, probes 3 cm long were needed to cover at least 30% of the sapwood depth in trees larger than 45 cm. For each individual monitored, two sensors were installed circumferentially at least 90° apart. Probes were installed, shielded from thermal gradients, and wired to dataloggers as described by Ford and Vose (2007). We replaced sensors if null, out of range, or negative readings were recorded, or if probes were physically damaged. Dataloggers queried sensors every 30 s, and logged 15-min means (Model CR10X, Campbell Scientific, Logan, Utah, USA). The temperature difference between the upper and lower probes was converted to sap flux density using a power equation similar in form to that of Granier (1985), but with coefficients derived on-site for each species (C. Ford, unpublished data). Maximum temperature differences for each sensor pair were identified during the previous two weeks. For all trees, readings for the two replicate sets of sensors were averaged. To scale  $J_s$  measurements made in the outer 2 or 3 cm of sapwood to total sap flow ( $F$ ,  $\text{g H}_2\text{O/s}$ ), we used a known radial profile for eastern

hemlock (Ford and Vose 2007) and developed a general radial profile for all other species using a measured profile for red maple, because species with similar xylem anatomy often display similar distributions of  $J_s$  within the functional xylem (Phillips et al. 1996). Methods are presented in Ford et al. (2007).

#### *Allometry and scaling*

We estimated sapwood area by extracting increment cores from nearby trees or from allometric relationships between over-bark dbh and sapwood area (SWA) determined from whole-tree harvests. Equations for red maple ( $n = 11$ ) and sweet birch ( $n = 10$ ) were developed from extracting increment cores from trees in the Coweeta basin at a nearby site (R. Hubbard and B. Kloeppel, unpublished data). Equations for rhododendron ( $n = 10$ ) were developed from extracting two increment cores per shrub on individuals growing adjacent to the study plots. SWA for *T. canadensis* was estimated from allometric equations (Santee 1978, Santee and Monk 1981). All trees and shrubs in the plots were surveyed for dbh in the winter months.

Peak leaf area for individual trees and shrubs was estimated using allometric equations relating leaf area to diameter at breast height (dbh). Equations for eastern hemlock were developed from 13 harvested trees at Coweeta, 10 of which spanned a range of dbh up to 26 cm harvested in 1970 (Santee 1978, Santee and Monk 1981), and three larger trees (37.7–57.1 cm dbh) from riparian areas harvested in late summer 2005 (C. Ford, unpublished data). Equations for rhododendron were developed from destructively harvested shrubs in the Coweeta basin that were growing along a low-elevation riparian corridor ( $n = 8$ ; Kloeppel et al., unpublished data). Equations for red maple and sweet birch were developed from destructively harvested trees in the Coweeta basin (Martin et al. 1999). Seasonal leaf area dynamics of *A. rubrum*, *B. lenta*, and *R. maximum* were monitored on six nearby individuals of each species during 2007 to determine the timing of peak leaf area (see Appendix). For each individual tree, two replicate leaves were monitored for budburst; after budburst, length and width of individual leaves were measured on a weekly basis until leaf size peaked. We used a different approach for eastern hemlock. Infestation with hemlock woolly adelgid was first documented on eastern hemlock in the basin in the late fall of 2005 and eastern hemlock did not produce a new foliage cohort in 2006 on the trees monitored. We used litter trap data collected on nearby plots to estimate timing of leaf fall for this species (Nuckolls 2007). For both eastern hemlock and the three replacement species, we estimated projected leaf area over time for each tree by multiplying the peak projected leaf area by the fraction of peak leaf area vs. day of year. These data were incorporated into the analysis of sap flux data to estimate leaf-level transpiration ( $E_L$ ) for individual trees. Mean daytime leaf-level transpiration rates were compared among species using



ANOVA for each of four seasons, spring (April–June), summer (July–September), autumn (October–December), and winter (January–March). Zero values before and after leaf-off were included in calculating mean  $E_L$  values for deciduous species in spring and autumn. Mean seasonal  $E_L$  values for individual trees and shrubs were used as replicates (red maple,  $n = 3$ ; sweet birch,  $n = 7$ ; rhododendron,  $n = 6$  and hemlock,  $n = 16$ ) in the analysis. Tukey tests were performed to test for significant differences between species pairs.

#### Data analysis

We used a Jarvis-type model to predict  $E_L$  from simultaneous effects of multiple climate variables, each having specific relationships to transpiration that may be either linear or nonlinear (Jarvis 1976, Granier and Loustau 1994). We initially tested whether  $E_L$  responded to four independent environmental parameters ( $T$ ,  $D$ , PPFD, and SMD), and developed a best-fit predictive model for each species and each parameter. To isolate the effect of each environmental parameter on  $E_L$  from effects of other variables, we used only data when other variables were not limiting to leaf gas exchange (Jarvis 1976). For example, to isolate the  $E_L$  response to  $D$ , we used only values when temperatures were 20–27°C, PPFD was  $>400 \mu\text{mol photons}\cdot\text{m}^{-2}\cdot\text{s}^{-1}$ , and SMD was 0.20–0.70. For rhododendron, relationships between  $E_L$  and  $D$ ,  $T$ , and PPFD were tested against climate data from both understory and open-field climate station sensors. Temperature was first eliminated from the analysis because, although it was a good predictor of  $E_L$  (e.g.,  $R^2 > 0.50$ ), it was highly correlated with  $D$ . Soil moisture deficit was also eliminated from the analysis because, although relationships were statistically significant, no best-fit relationships between  $E_L$  and SMD explained more than 4% of the variation in  $E_L$ . The lack of effect of soil moisture on  $E_L$  may be the result of the landscape position of the plots used in the study, because all sites were in riparian zones where soil moisture deficit is less intense than in more mesic mid-slope sites or xeric ridges. We used a linear equation in the  $E_L$  response to  $D$  (Eq. 3) for all species except sweet birch, where we used a natural log equation. We used a natural log equation for  $f$  in the  $E_L$  response to PPFD (Eq. 4) for all species:

$$E_L = \beta_1 \times D + \beta_2 \quad (2)$$

$$E_L = \beta_3 \times \ln(\text{PPFD}) + \beta_4. \quad (3)$$

Parameter estimates for equations relating  $E_L$  to single environmental variables (e.g.,  $\beta_1$ ,  $\beta_2$ ) were obtained using SigmaPlot (version 11.0, Systat, Chicago, Illinois, USA). These parameter estimates for single-factor regression models then served as “seed values” (i.e., they provided a starting point for the parameter estimates during the iteration process) for fitting the final model using a nonlinear mixed-model approach with individual trees acting as replicates (Peek et al.

2002), as follows:

$$y = f(x_{ij}, \beta, u_i) + e_{ij} \quad (4)$$

where  $f$  is a function of: covariates ( $x_{ij}$ , e.g.,  $D$ , PPFD) for the  $j$ th observation (day) on the  $i$ th individual (tree or shrub), fixed-effects parameters ( $\beta$ , e.g., species), and an unknown vector of random effect parameters ( $u_i$ ). Random errors are unknown and denoted as  $e_{ij}$ . The  $u_i$  term was incorporated to account for repeated measurements in time, and assumes that errors are not independent. Combined models were fit using PROC NLMIXED in SAS software (version 9, SAS Institute, Cary, North Carolina, USA). We repeated this procedure for each species and also developed a generic model for all other deciduous species using data from sweet birch and red maple (henceforth “generic”), resulting in a total of five models. Models for each species were parameterized using data from April 2006–September 2008 minus validation data. The final model for red maple, rhododendron, and the generic deciduous species took the following form:

$$E_L = (\beta_1 \times D + \beta_2) \times [\beta_3 \times \ln(\text{PPFD}) + \beta_4] \times \beta_7. \quad (5)$$

The final model for sweet birch took the form:

$$E_L = [\beta_1 \times \ln(D) + \beta_2] \times [\beta_3 \times \ln(\text{PPFD}) + \beta_4] \times \beta_7. \quad (6)$$

Validation data were selected systematically during the early (mid-May), middle (early July), and late (early September) growing seasons among all years and were selected to represent the broadest range of both  $D$  and PPFD values observed during those periods. For each period, five consecutive days were selected for ~300 data points. Observed and predicted values of  $E_L$  were compared using simple linear regression. Annual stand  $E_t$  was then determined by summing all  $E_L$  values for each species (during the growing season for deciduous species, and during the entire year for rhododendron) and scaling  $E_L$  to stand  $E_t$  using projected leaf area for that species.

#### Model application

Species-specific response models were used to estimate total stand  $E_t$  from 2004–2011 and forecast potential future  $E_t$  through 2050. Equations for  $E_L$  for red maple, sweet birch, and rhododendron were used to estimate water use of those species and the generic deciduous tree species was used to estimate  $E_L$  for the remaining species. Mean values of  $D$  and PPFD, observed every 15 minutes from 2006–2008, were used as input for climate for all years and only LAI varied through time. We used allometric equations to estimate sapwood area and projected leaf area from dbh. Although year-to-year estimates of leaf area based on allometry can be coarse, these estimates were not outside of the bounds of variation in estimates of projected leaf area based on litterfall collected in the same plots from 2004 to 2011

TABLE 1. Observed (2004 and 2011) and forecasted (2020–2050) basal area (BA), sapwood area (SWA), and leaf area index (LAI) for red maple, sweet birch, rhododendron, eastern hemlock, and all other species in plots during the course of hemlock loss and replacement by deciduous species.

Species and year	BA (cm <sup>2</sup> /m <sup>2</sup> )	SWA (cm <sup>2</sup> /m <sup>2</sup> )	LAI (m <sup>2</sup> /m <sup>2</sup> )
<b>Red maple</b>			
2004	0.59	0.46	0.13
2011	0.75	0.56	0.16
2020	1.28	1.00	0.21
2030	1.44	1.14	0.23
2040	1.55	1.23	0.24
2050	1.63	1.30	0.24
<b>Sweet birch</b>			
2004	3.73	2.39	0.73
2011	4.88	3.13	0.97
2020	8.44	6.03	1.26
2030	9.50	6.85	1.34
2040	10.19	7.37	1.40
2050	10.69	7.76	1.44
<b>Rhododendron</b>			
2004	4.56	2.11	0.80
2011	4.82	2.40	0.86
2020	8.37	4.38	1.11
2030	9.39	4.97	1.19
2040	10.06	5.35	1.23
2050	10.55	5.63	1.27
<b>Hemlock</b>			
2004	31.28	18.06	4.41
2011	0	0	0
2020	0	0	0
2030	0	0	0
2040	0	0	0
2050	0	0	0
<b>Other</b>			
2004	12.34	5.08	2.17
2011	12.06	5.04	1.96
2020	21.10	9.23	2.55
2030	23.52	10.41	2.71
2040	25.08	11.18	2.82
2050	26.24	11.74	2.90
<b>Total</b>			
2004	52.50	28.03	7.98
2011	22.52	15.55	3.94
2020	39.19	20.65	5.13
2030	43.86	23.37	5.46
2040	46.87	25.12	5.69
2050	49.10	26.43	5.85

Notes: SWA and LAI values in 2004 and 2011 are based on allometric relationships of sapwood area and projected leaf area to diameter at breast height (1.37 m) on a healthy tree. Forecasted BA, SWA, and LAI values are based on a natural log model fitted to observed increases in tree growth after 2007, and were assumed to peak at a stand maximum of 50.0 cm<sup>2</sup>/m<sup>2</sup> (BA), 28 cm<sup>2</sup>/m<sup>2</sup> (SWA), and 6.0 m<sup>2</sup>/m<sup>2</sup> (LAI), based on survey data from nearby deciduous forest plots.

(Nuckolls 2007, Knoepp et al. 2012; J. Knoepp, unpublished data). To forecast changes in community composition, we developed equations for each species to predict future basal area, sapwood area, and projected leaf area (Table 1) by fitting natural log functions to changes in those parameters observed between 2007 (when hemlock mortality reached >50%) and 2011.

Based on the structure of nearby hardwood stands (S. Brantley, unpublished data), we assumed that total stand basal area would peak at ~50 cm<sup>2</sup>/m<sup>2</sup>, sapwood area would peak at ~28 cm<sup>2</sup>/m<sup>2</sup>, and stand leaf area index would peak at ~6.0 m<sup>2</sup>/m<sup>2</sup>. Annual stand  $E_L$  for each year was determined by integrating all  $E_L$  values for each species (during the growing season for deciduous species, and during the entire year for rhododendron) and scaling  $E_L$  to stand  $E_L$  using projected leaf area for that species.

## RESULTS

### Climate

Annual precipitation was 1550 mm in 2006, 1212 mm in 2007, and 1516 mm in 2008. These were 14%, 32%, and 16% lower than the long-term mean of 1794 mm recorded in the basin through 2011, and, consequently, were all relatively dry years. Soil moisture deficit was similar among years, averaging 0.51 (equivalent to ~25% volumetric water content) and reaching 1 (10% volumetric water content) during August 2006 (Fig. 1). Soil moisture deficit was generally highest during the growing season and declined only with precipitation events with >30 mm daily rainfall (Fig. 1), but this response also depended on season and antecedent precipitation. Midday, above-canopy PPFD ranged from ~1300 to >2000  $\mu\text{mol photons}\cdot\text{m}^{-2}\cdot\text{s}^{-1}$  on clear days, whereas midday below-canopy PPFD ranged from 11 to 332  $\mu\text{mol photons}\cdot\text{m}^{-2}\cdot\text{s}^{-1}$  (Fig. 1). Daily cumulative above-canopy PPFD peaked in early June. Understory PPFD peaked in early to mid-April before canopy leaf development, and rapidly declined after canopy budbreak (Fig. 1). Midday temperatures were 4.7°C lower, on average, in the understory than in the open. Vapor pressure deficit varied from 0 to 3.99 kPa and was tightly coupled with temperature. Vapor pressure deficit approached zero most mornings and was lower, on average, beneath the canopy by 0.56 kPa.

### Stand composition and structure

Over the course of the study period, hemlock mortality was nearly complete and a mix of red maple, yellow poplar, sweet birch, and rhododendron had positively responded across all plots (Table 1). In 2004, hemlock represented 61% of the basal area, 64% of the sapwood area, and 55% of the leaf area in the four intensively monitored hemlock plots. By 2011, live hemlock basal area, sapwood area, and projected leaf area had been reduced >99%. Only three small live trees remained in 2011 and those had a very sparse green canopy because new leaf cohorts had not been produced since 2005 (Nuckolls 2007). In the same period, basal area for red maple increased 22%, sweet birch increased 24%, rhododendron increased 6%, and yellow poplar increased 27%. As a group, other species had declined in basal area by 11%, primarily due to mortality of a few large trees. As of December 2011, sweet birch had the highest basal area (21.0%), followed by rhododendron

(20.7%) and yellow poplar (17.8% basal area). The remaining basal area was represented by a mix of hardwood and evergreen species, with red maple (4% basal area) as the only other species occurring in all study plots.

#### Transpiration rates

Our first goal was to determine if the deciduous species replacing hemlock had higher  $E_L$  rates than hemlock during the growing season. We hypothesized that *A. rubrum* and *B. lenta* would have higher transpiration rates, with *R. maximum* having similar rates to *T. canadensis*; this hypothesis was supported by our sap flux measurements. Measured  $E_L$  ( $\text{mmol H}_2\text{O}\cdot\text{m}^{-2}\cdot\text{s}^{-1}$ ) varied significantly among species during spring, summer, and autumn (all  $P < 0.001$ ), but did not vary between hemlock and rhododendron during winter ( $P = 0.882$ ) (Fig. 2). Mean daytime  $E_L$  in summer ranged from  $0.110 \text{ mmol H}_2\text{O}\cdot\text{m}^{-2}\cdot\text{s}^{-1}$  for eastern hemlock prior to infestation (i.e., 2004–2005) to  $0.605 \text{ mmol H}_2\text{O}\cdot\text{m}^{-2}\cdot\text{s}^{-1}$  for sweet birch. Sweet birch  $E_L$  was significantly higher than all other species in all seasons except winter, whereas red maple  $E_L$  was significantly higher than hemlock during spring and summer (Fig. 2). Mean  $E_L$  for rhododendron and hemlock did not differ significantly during any period (Fig. 2). For example, mean  $E_L$  values during autumn and winter for rhododendron were  $0.095$  and  $0.101 \text{ mmol H}_2\text{O}\cdot\text{m}^{-2}\cdot\text{s}^{-1}$ , respectively, compared to  $0.095$  and  $0.097 \text{ mmol H}_2\text{O}\cdot\text{m}^{-2}\cdot\text{s}^{-1}$  for hemlock.

Leaf-level transpiration was significantly related to measured climate variables (Fig. 3). Open-field  $D$  was the best single predictor of  $E_L$  for all canopy species (Fig. 3). Relationships between rhododendron  $E_L$  and  $D$  were marginally better using understory  $D$  ( $R^2 = 0.70$  vs.  $R^2 = 0.65$ ); however, open-field climate data were used to construct the model so that future modeling can use data from the climate station. Light was the second-best predictor of  $E_L$  (Fig. 3). Open-field PPFD was better at predicting  $E_L$  in rhododendron than was understory PPFD ( $R^2 = 0.31$  and  $0.20$ , respectively); thus, above-canopy PPFD was used in the models for all three species. As a result of the variations in transpiration rates and species-dependent responses to environmental factors, each species required a unique model to estimate  $E_L$  from  $D$  and PPFD (Tables 2 and 3). We were able to predict >80% of variation in  $E_L$  for all species (Fig. 4, Table 3). Relationships between modeled and observed data were close to 1:1; and when validation  $E_L$  data were integrated over time, there was <2% difference between observed and predicted  $E_L$  for all species (Fig. 4, Table 3).

Our second goal was to determine the potential changes in annual and seasonal patterns of  $E_t$  from eastern hemlock loss. Although hemlock had conservative rates of  $E_L$ , it was still the largest contributor to annual stand  $E_t$  before HWA infestation. Integrating  $E_L$  over an entire year and scaling the contribution of each

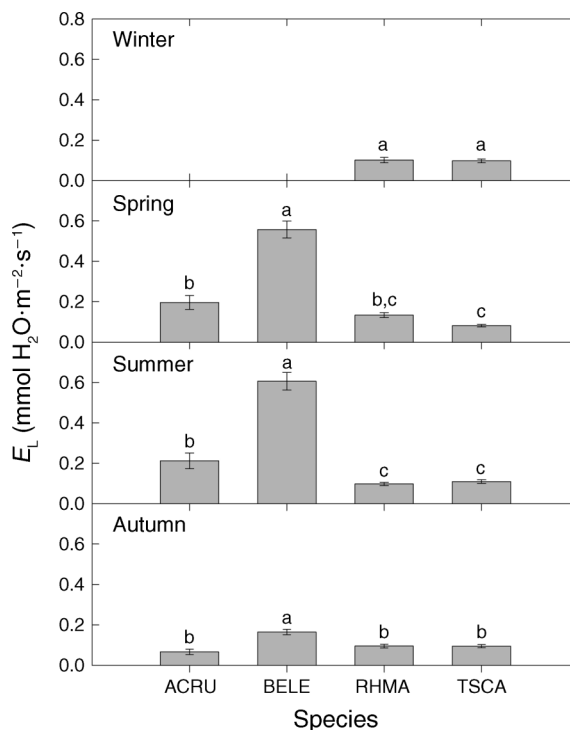


FIG. 2. Leaf-level transpiration rates,  $E_L$  (mean  $\pm$  SE), for each species by season: ACRU, *Acer rubrum*; BELE, *Betula lenta*; RHMA, *Rhododendron maximum*; and TSCA, *Tsuga canadensis*. Mean values for deciduous species (*A. rubrum* and *B. lenta*) include days for spring (before bud burst) and autumn (after leaf-off) when  $E_L$  was zero. Significant differences ( $P < 0.05$ ) among species during each season are noted by different lowercase letters.

species using stand-level LAI values from 2004–2006, observed annual stand  $E_t$  for 2004–2006 was  $633 \pm 9 \text{ mm}$  (mean  $\pm$  SE; Fig. 5). Annual stand  $E_t$  declined to  $494 \text{ mm}$  by 2011 due to hemlock mortality (Fig. 5). Hemlock was the largest single component of  $E_t$  for these stands, with  $164 \text{ mm/yr}$ , or 25.9% of the total stand  $E_t$  prior to infestation. Sweet birch comprised much less leaf area than hemlock (Table 1), but it accounted for  $143 \text{ mm/yr}$  (23.1%) of total stand  $E_t$ . The rhododendron component accounted for  $59.7 \text{ mm/yr}$  (9.6%), and red maple accounted for  $7.9 \text{ mm/yr}$  (1.3%). For these stands, species rank of annual water use from 2004–2006, from highest to lowest, was hemlock > sweet birch > rhododendron > red maple. Other species contributed  $240.2 \text{ mm/yr}$  (38.8%) to total  $E_t$ . Autumn and winter  $E_t$  together represented 18.6% of annual  $E_t$  and ~60% of that was from hemlock. The contribution of hemlock to total winter  $E_t$  was  $39.6 \text{ mm/yr}$ , or 74% of  $53.3 \text{ mm/yr}$ , with the remainder of winter  $E_t$  coming from rhododendron. A similar pattern was observed in autumn: hemlock contributed  $32.2 \text{ mm/yr}$ , or 52% of  $E_t$ , rhododendron contributed  $15.8 \text{ mm/yr}$ , and deciduous species contributed  $14.1 \text{ mm/yr}$  of the total autumn  $E_t$  of  $62.1 \text{ mm/yr}$ . Winter  $E_t$  had declined to  $13.7 \text{ mm/yr}$  by

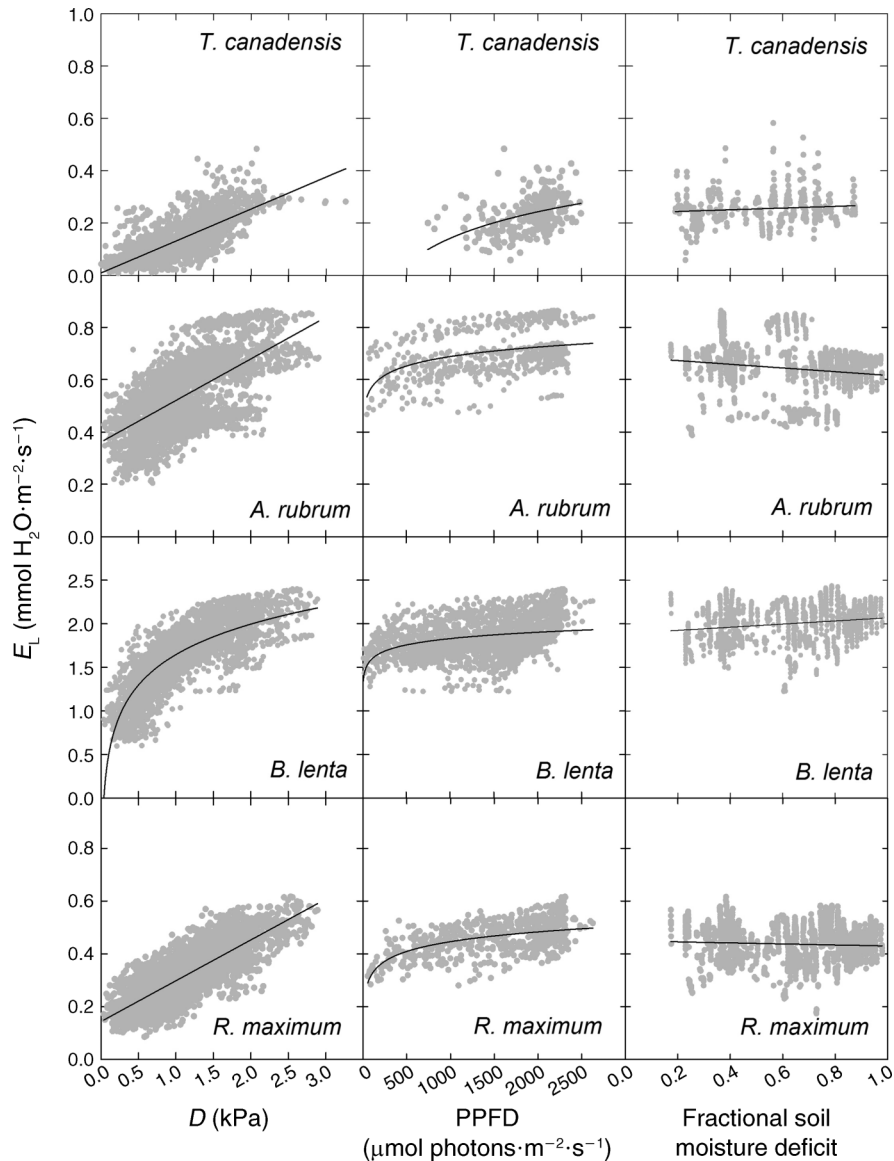


FIG. 3. Observed responses of transpiration per unit leaf area ( $E_L$ ) to individual climate parameters under non-limiting conditions to all other climate variables for *Tsuga canadensis* (eastern hemlock), *Acer rubrum* (red maple), *Betula lenta* (sweet birch), and *Rhododendron maximum* (rhododendron). Best-fit regression lines are shown for either linear or natural log functions.

TABLE 2. Model coefficients and coefficients of determination ( $R^2$ ) for relationships between transpiration per unit leaf area ( $E_L$ ) and single environmental variables (air vapor pressure deficit,  $D$ ; photosynthetic photon flux density, PPFD; and soil moisture deficit, SMD) for four species and a generic deciduous tree species.

Species	$\beta_1$	$\beta_2$	$R^2$	$\beta_3$	$\beta_4$	$R^2$	$\beta_5$	$\beta_6$	$R^2$
Hemlock	0.1224	0.0083	0.5825	0.1457	-0.8645	0.162	0.0327	0.2370	0.001
Red maple	0.1589	0.3613	0.396	0.0524	0.3257	0.152	-0.0705	0.6868	0.018
Sweet birch	0.5048	1.645	0.656	0.1054	1.1009	0.115	0.1803	1.8875	0.027
Rhododendron	0.1545	0.1436	0.659	0.0532	0.0784	0.311	-0.0196	0.4494	0.002
Generic tree sp.	0.3364	0.7104	0.088	0.0962	1.1624	0.100			

Notes: Equations are  $E_L = \beta_1 \times D + \beta_2$  (for red maple, rhododendron, and the generic species) or  $E_L = \beta_1 \times \ln D + \beta_2$  (for sweet birch),  $E_L = \beta_3 \times \ln PPFD + \beta_4$  (for all species), and  $E_L = \beta_5 \times SMD + \beta_6$  (for all species), where  $E_L$  is  $\text{mmol H}_2\text{O}\cdot\text{m}^{-2}\cdot\text{s}^{-1}$ ,  $D$  is kPa, PPFD is  $\mu\text{mol photons}\cdot\text{m}^{-2}\cdot\text{s}^{-1}$ , and SMD is fractional. Model coefficients were used as “seed values” (providing a starting point for parameter estimates during the iteration) for final model parameterization, which incorporated only  $D$  and PPFD; SMD was not used due to low  $R^2$  values. The relationship between  $E_L$  and SMD was not tested for the generic species.



TABLE 3. Coefficient estimates ( $\pm$ SE) for a nonlinear mixed model using  $D$  and PPFD to predict  $E_L$  and results of comparisons between observed and predicted  $E_L$  values.

Species	$\beta_1$	$\beta_2$	$\beta_3$	$\beta_4$	$\beta_7$	$R^2$	Error
Hemlock	0.7503 <sup>a</sup> (0.0324)	0.1224 <sup>a</sup> (0.0023)	0.0229 <sup>a</sup> (0.0012)	-0.0534 <sup>a</sup> (0.0047)	1.4523 <sup>a</sup> (0.1343)	0.817	+0.4%
Red maple	1.0973 <sup>b</sup> (0.0085)	0.2228 <sup>b</sup> (0.0027)	0.3613 <sup>b</sup> (0.0042)	0.0133 <sup>b</sup> (0.0011)	0.5957 <sup>b</sup> (0.0353)	0.818	-1.7%
Sweet birch	0.3253 <sup>c</sup> (0.0016)	0.3362 <sup>c</sup> (0.0012)	2.4084 <sup>c</sup> (0.0036)	0.0788 <sup>c</sup> (0.0015)	1.5357 <sup>a</sup> (0.0418)	0.812	+1.3%
Rhododendron	0.4780 <sup>d</sup> (0.0044)	0.1075 <sup>d</sup> (0.0006)	0.7012 <sup>d</sup> (0.0024)	0.0462 <sup>d</sup> (0.0012)	0.5687 <sup>b</sup> (0.0227)	0.822	-0.3%
Generic tree sp.	0.6245 <sup>e</sup> (0.0068)	0.3516 <sup>e</sup> (0.0063)	0.7104 <sup>d</sup> (0.0165)	0.0327 <sup>c</sup> (0.0029)	1.1624 <sup>c</sup> (0.0409)		

Note: The model took the form:  $E_L = (\beta_1 \times D + \beta_2) \times (\beta_3 \times \ln \text{PPFD} + \beta_4) \times \beta_7$ , where  $E_L$  is in units of  $\text{mmol H}_2\text{O} \cdot \text{m}^{-2} \cdot \text{s}^{-1}$ ,  $D$  is in units of kPa, and PPFD is in units of  $\mu\text{mol photons} \cdot \text{m}^{-2} \cdot \text{s}^{-1}$ . Significant differences ( $P < 0.05$ ) in the coefficients among species are noted with superscript letters within a column. Values for  $R^2$  are the result of comparisons between observed  $E_L$  and  $E_L$  predicted by the model for each species. Percentage error is the difference between observed  $E_L$  and  $E_L$  predicted by the model over the entire study period. For the generic species, no comparison could be made between observed and predicted values.

2011 due to hemlock loss (Fig. 5). This represented a change from 8.6% of total annual  $E_t$  to only 2.8% of annual  $E_t$ . Similarly, autumn  $E_t$  (October–December) declined to 32.9 mm/yr, 53% of pre-HWA levels, by 2011.

#### Model applications

Results of our simulations suggest that annual  $E_t$  is expected to recover to pre-infestation levels due to replacement by deciduous species, but winter and autumn  $E_t$  will remain suppressed throughout the simulation period due to a relatively weak response by rhododendron (Fig. 5). Under current averages for PPFD and  $D$ , forecasted increases in LAI result in

annual stand  $E_t$  recovering to 2004 values (i.e., pre-infestation) by  $\sim 2020$ . By 2050,  $E_t$  is projected to reach 706 mm/yr under current climatic conditions, which is a 12% increase in  $E_t$  over pre-HWA levels and represents  $\sim 40\%$  of current annual precipitation. However, winter  $E_t$  does not recover to 2004 levels. Simulated winter  $E_t$  reaches only 20.1 mm/yr (38% of 2004 values) by 2050, and is projected to represent only 2.8% of total annual  $E_t$  by that time. Similarly, autumn  $E_t$  only recovers to 45.0 mm/yr ( $\sim 73\%$  of pre-HWA  $E_t$ ) by 2050. Rhododendron is forecasted to represent nearly 100% of winter  $E_t$  and 44% of autumn  $E_t$  by 2050; thus, rhododendron may have an important role in affecting seasonal patterns of  $E_t$ , but rhododendron LAI in these stands

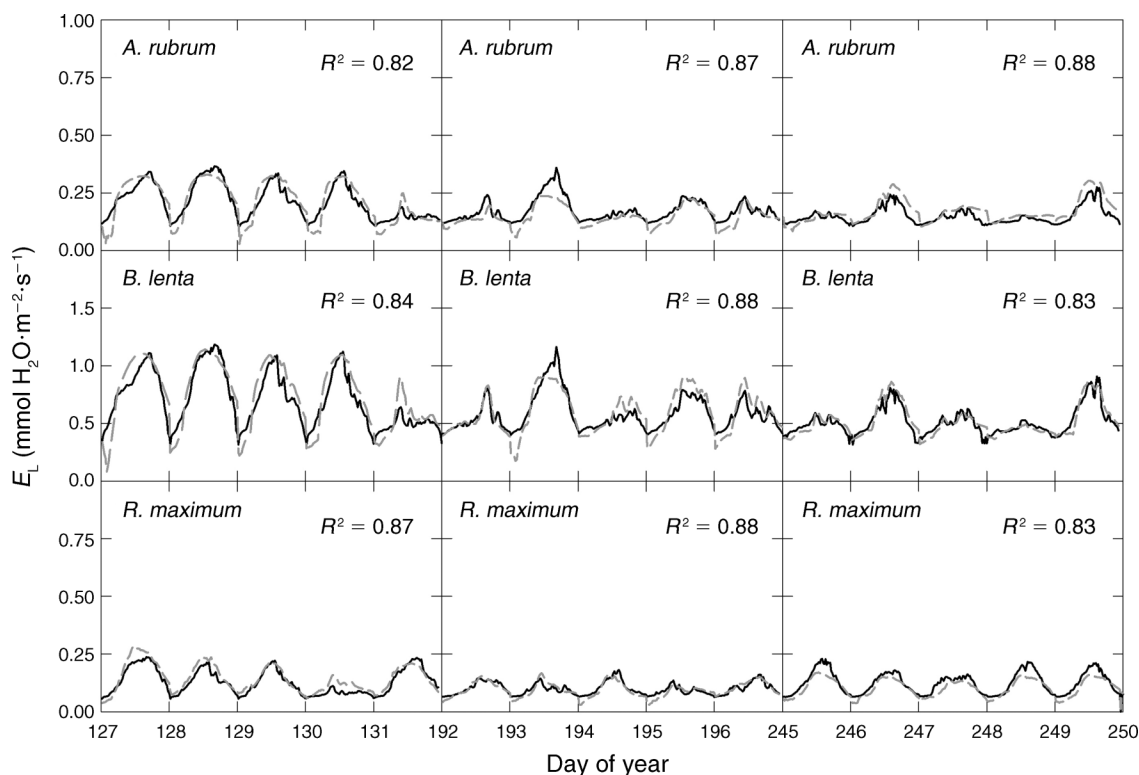


FIG. 4. Comparison of observed (solid black line) and predicted (dashed gray line) leaf-level transpiration ( $E_L$ ) for spring, summer, and autumn validation periods during 2006 for *A. rubrum*, *B. lenta*, and *R. maximum*.  $R^2$  values indicate results of a best-fit linear regression for the period shown.

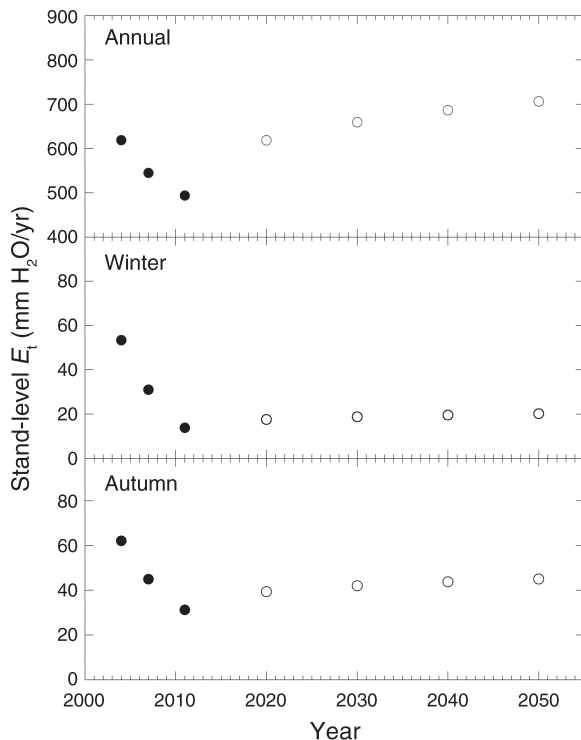


FIG. 5. Observed (2004–2011, solid circles) and forecasted (2020–2050, open circles) stand-level  $E_t$  for intensive hemlock plots infested with hemlock woolly adelgid in 2004. Annual, winter (January–March), and autumn (October–December)  $E_t$  are shown.

was not stimulated enough to compensate for the large reduction in LAI from hemlock loss.

#### DISCUSSION

Measured transpiration rates varied significantly among hemlock, sweet birch, red maple, and rhododendron for all time scales measured. Sweet birch, in particular, had a much higher daily and instantaneous  $E_L$  than red maple, rhododendron, or hemlock. Although hemlock demonstrated a very conservative  $E_L$  compared to other species, it represented about one-fourth of stand  $E_t$  prior to HWA infestation because it contributed so greatly to stand basal area and the evergreen leaf phenology allowed year-round transpiration. As a result, stand  $E_t$  declined sharply as hemlock mortality progressed from 2004 to 2011, particularly in 2007 when hemlock mortality accelerated, and again in 2011 when mortality in the study plots neared 100%. As a result of hemlock mortality, the percentage of annual precipitation that was accounted for by  $E_t$  declined from ~35% prior to hemlock infestation to ~28% after hemlock loss. The decline in annual  $E_t$  is expected to be temporary, and annual  $E_t$  will probably increase above pre-HWA levels as hemlock is replaced by species with less conservative  $E_L$  rates.

Future changes in annual forest  $E_t$  in these stands will depend heavily on the species composition of the community that replaces hemlock. Although it is difficult to predict species composition of these stands in the next 40–50 years accurately, several species, especially rhododendron, sweet birch, and yellow poplar, showed large, positive growth responses to hemlock mortality, particularly after 2007. Enhanced growth relative to undisturbed sites was probably a result of changes in light in the lower canopy, which increased immediately after hemlock canopy loss (Ford et al. 2012). Other factors, including soil moisture and soil nutrient pools, did not respond in the years immediately after hemlock infestation and are less likely to have had an impact on species responses (Ford et al. 2012, Knoepp et al. 2012). Existing sweet birch trees demonstrated a particularly strong positive growth response to hemlock loss, which is not surprising considering that this species is known to take advantage of light gaps common with canopy disturbances (Ward and Stephens 1996, Carlton and Bazaaz 1998).

As a result of the rapid growth response of co-occurring species, and changes in  $E_t$  from replacement by species with less conservative  $E_L$ , our results suggest that annual  $E_t$  will recover from hemlock loss by around 2020. Perhaps of more interest is that beyond 2020, loss of hemlock may result in a substantial increase in forest  $E_t$ , compared to pre-HWA levels. Several authors have suggested that a transition from hemlock to deciduous species in New England hemlock stands will stimulate annual forest  $E_t$  (Catovsky et al. 2002, Daley et al. 2007, Hadley et al. 2008). Daley et al. (2007) specifically noted an increase in  $E_t$  after replacement of hemlock with sweet birch, the dominant response in New England hemlock stands (Ellison et al. 2005). Unlike the stands in Massachusetts studied by Daley et al. (2007), sweet birch is near the southern end of its range at our study site. In the southern Appalachians, sweet birch leafs out in early spring, is subject to a longer growing season, and experiences higher summer temperatures than sweet birch in the northeastern United States. Therefore, the stimulation in  $E_t$  resulting from an increase in sweet birch leaf area and sapwood area in the southern Appalachians may be even more pronounced than in the northeastern United States, and this could lead to a much greater effect on growing-season soil moisture and stream discharge.

Assuming that growth response of existing trees continues on the current trajectory, sweet birch and rhododendron are likely to be the largest contributors to stand  $E_t$  in the future, with red maple and yellow poplar as other major contributors. Although yellow poplar  $E_L$  was not measured in the current study, it may also become a large contributor to stand  $E_t$  in future because it has relatively high  $E_L$  rates, very similar to those of sweet birch (Ford et al. 2011b; S. Brantley, *unpublished data*). On the other hand, the future contribution of red maple to stand  $E_t$  may be limited by lack of new

recruitment because of suppression by rhododendron. Although red maple is the single most common tree in low-elevation sites in our study area (Elliott and Swank 2008), is present in all plots in this study, and its growth responded positively to hemlock loss (Ford et al. 2012), it did not represent a large proportion of leaf area in these stands before HWA infestation. Because rhododendron suppresses tree seedling recruitment in the southern Appalachians (Clinton and Vose 1996, Lei et al. 2002), the prevalence of rhododendron could lessen the potential future contribution of tree species, such as *A. rubrum*, that do not already represent a substantial component of leaf area in these stands.

Stimulation of  $E_t$  through replacement with species such as *B. lenta* and *L. tulipifera* might also change the relationship between  $E_t$  and soil moisture. Although all species responded strongly to  $D$ , with PPFD serving as a secondary predictor of  $E_L$ , soil moisture deficit did not enhance our ability to predict  $E_L$  in any of the species. Soil moisture deficit was seemingly not important for these trees over our study period, even in the three relatively dry years during the course of sap flux density measurements, with 2007 being particularly dry. The lack of response may be primarily a result of the landscape position. All of these plots were located in riparian areas with convergent topography; and while soil moisture deficit reached 1 in the growing season, mean seasonal soil moisture never fell below 20% (volume/volume) in these stands (Ford et al. 2012). Rhododendron would most likely be the first species affected by drier soils because of shallow roots, but rhododendron is also most likely to be found streamside (Narayanaraj et al. 2009).

Although annual  $E_t$  is predicted to recover from hemlock mortality in  $\sim 10$  years, seasonal patterns of  $E_t$  are predicted to be altered permanently compared to hemlock-dominated stands because the species expected to replace hemlock are primarily deciduous. Unlike hemlock and rhododendron, water use by sweet birch, yellow poplar, and red maple is limited by leaf phenology. Recovery of autumn and winter  $E_t$  from replacement by rhododendron, which has seasonal patterns of  $E_L$  most similar to hemlock, appeared unlikely. Although rhododendron winter  $E_L$  rates were higher than hemlock, and rhododendron growth responded positively to canopy loss, the increase in rhododendron leaf area was relatively small compared to the leaf area lost from hemlock mortality. Replacement of hemlock with deciduous species means that stand LAI is likely to reach a maximum sustainable level well below LAI values observed before HWA infestation. Typically, deciduous stands in the Coweeta basin reach a maximum LAI of  $\sim 6$  compared the 8–10 observed in hemlock stands (Vose et al. 1995, Ford et al. 2011b). The lack of leaf area stimulation resulted in a relatively slow increase in the role of rhododendron in annual forest  $E_t$ , and rhododendron is unlikely to serve

as a functional replacement for hemlock in autumn and winter.

Although rhododendron will not replace hemlock functionally under current climate conditions, the relative importance of rhododendron, and other evergreens, to forest  $E_t$  may increase in the future as a result of warming, especially in winter. Mean annual temperature has increased in the Coweeta basin  $\sim 0.5^\circ\text{C}$  per decade since the early 1980s (Laseter et al. 2012), and is expected to continue to increase in the future (IPCC 2007). The effects of warming on forest evaporative demand are complex, often depending on interactions with other factors such as  $\text{CO}_2$  enrichment (Medlyn et al. 2001, Katul et al. 2009, Warren et al. 2011), changes in phenology, and increased drought frequency. For example, evergreen species with sclerophyllous leaves, such as rhododendron, probably will benefit more from increasing  $\text{CO}_2$  than will deciduous species or species with non-complex leaf venations, due to effects on mesophyll conductance (Niinemets et al. 2009). As a consequence, results to date regarding the effects of climate change on forest  $E_t$  are mixed and often contradictory (Labat et al. 2004, Walter et al. 2004, Hänninen and Tanino 2011). For rhododendron specifically, the effects of warmer temperatures in winter may include an increase in stomatal conductance and reduced leaf damage (Hall 2008, Russell et al. 2009). Direct effects of future increases in  $D$  may also stimulate winter  $E_t$ , but much of this depends on how humidity responds to warming. Specific humidity is expected to increase as temperature increases (Allen and Ingram 2002, Held and Soden 2006), but if temperatures increase without concurrent increases in specific humidity, greater  $D$  values during winter could stimulate  $E_t$  in evergreens and increase water use during winter.

#### Applications

Hemlock is heavily concentrated in riparian areas, where it may represent  $>50\%$  of basal area. Areas that lose hemlock may demand active management strategies if restoration of stand-level transpiration is desirable. Historically, the widespread loss of a species as important as eastern hemlock has not occurred in the southern Appalachians since *Cryphonectria parasitica* (Murrill) Barr eradicated populations of American chestnut, *Castanea dentata* (Marsh.) Borkh. (Fagaceae), in the 1930s. Chestnut represented  $>30\%$  of basal area in southern Appalachian forests before the chestnut blight pandemic. Although hemlock represents a much smaller percentage of basal area ( $\sim 5\%$ ) across the entire landscape (Elliott and Swank 2008), hemlock is the dominant canopy tree in many riparian forests and plays an important role in regulating winter stream discharge (Ford and Vose 2007). Furthermore, increased annual water use from replacement with deciduous species is likely to reduce stream discharge during the late growing season; flow in some smaller streams may not be sustainable in birch-dominated stands (Daley et al.

2007). Although data are currently incomplete, monitoring HWA-mediated changes in discharge in the Coweeta basin will be an area of high interest in the future. To restore pre-HWA hydrologic function, restoration with eastern hemlock would be ideal if resistant varieties could be found and planted on a widespread basis. Otherwise, replacement of hemlock with other evergreen tree species that imitate the structure and function of hemlock would be advisable. In addition to the changes in  $E_t$  described in the current study, eastern hemlock loss probably will also alter canopy interception, especially in winter; replacement with another evergreen that has similar interception rates might be desirable. Care must be taken, however, with selection of species used to mitigate functional changes resulting from hemlock mortality. *Pinus strobus* (eastern white pine), for instance, has been suggested as a functional replacement for hemlock (Jonas et al. 2012) because it is an evergreen that can also sustain high LAI values similar to those observed in pre-HWA hemlock stands (Ford et al. 2011a) and provide shade and year-round evergreen cover. However, eastern white pine has a much less conservative instantaneous  $E_L$  and greater annual  $E_t$  than hemlock (Ford et al. 2011a); and although winter  $E_t$  patterns after replacement of hemlock with eastern white pine would more closely resemble pre-HWA  $E_t$  in hemlock stands, it might result in long-term increases in annual  $E_t$ .

Although hemlock is a relatively small component of the entire low-elevation southern Appalachian forest, it is densely concentrated in riparian and cove habitats and its local influence on microclimate, community composition, and nutrient cycling due to high LAI of hemlock stands is substantial. In addition to moderating stream discharge, hemlock stands are known for their cool, dark microclimates that contrast with surrounding forests (Orwig et al. 2012). The conservative  $E_L$  of hemlock probably contributed to the ability of these stands to maintain high LAI values that limited light penetration and contributed to this unique climate. As hemlock is replaced by species with higher  $E_L$ , a permanent reduction in leaf area will also lead to increases in understory light and soil temperature, decreases in litter layer moisture, and accelerated decomposition (Cobb et al. 2006, Spaulding and Rieske 2010, Orwig et al. 2012). These changes will eventually eliminate a unique habitat and increase landscape-level forest homogeneity. These factors will affect ecosystem function beneath dead and decaying eastern hemlock for decades to come, and will have important implications for riparian habitats beyond effects on stream discharge.

#### ACKNOWLEDGMENTS

This study was supported by the USDA Forest Service, Southern Research Station and by NSF grants DEB0218001 and DEB0823293 to the Coweeta LTER program at the University of Georgia. Any opinions, findings, conclusions, or recommendations expressed in the material are those of the authors and do not necessarily reflect the views of the National

Science Foundation or the University of Georgia. We are grateful to Stan Wullschleger and David Orwig for providing helpful comments on a previous version of this manuscript. We acknowledge the support of many individuals, past and present, as well as the long-term climate and hydrologic data network at Coweeta Hydrologic Lab, especially K. Bower, J. Davis, B. Kloeppel, S. Laseter, J. P. Love, R. McCollum, C. Marshall, N. Muldoon, J. Meador, and G. Zausen for fieldwork and climate data collection and processing.

#### LITERATURE CITED

- Adams, H., C. Luce, D. Breshears, C. Allen, M. Weiler, V. Cody, A. Smith Hale, and T. Huxman. 2012. Ecohydrological consequences of drought- and infestation-triggered tree die-off: insights and hypotheses. *Ecohydrology* 5:145–159.
- Allen, M., and W. Ingram. 2002. Constraints on future changes in climate and the hydrologic cycle. *Nature* 419:224–232.
- Brown, J. 2004. Impacts of hemlock woolly adelgid on Canadian and Carolina hemlock forests. Pages 19–36 in *Proceedings: Land use change and implications for biodiversity on the Highlands plateau: A report by the Carolina Environmental Program, Part A. Highlands Biological Station, Highlands, North Carolina, USA.*
- Campbell, G., and J. Norman. 1998. *Radiation basics: An introduction to environmental biophysics.* Springer-Verlag, New York, New York, USA.
- Carlton, G., and F. Bazaaz. 1998. Regeneration of three sympatric birch species on experimental hurricane blowdown microsites. *Ecological Monographs* 68:99–120.
- Catovsky, S., N. Holbrook, and F. Bazaaz. 2002. Coupling whole-tree transpiration and canopy photosynthesis in coniferous and broad-leaved tree species. *Canadian Journal of Forest Research* 32:295–309.
- Clinton, B., and J. Vose. 1996. Effects of *Rhododendron maximum* L. on *Acer rubrum* L. seedling establishment. *Castanea* 61:38–45.
- Cobb, R., D. Orwig, and S. Currie. 2006. Decomposition of green foliage in eastern hemlock forests of southern New England impacted by hemlock woolly adelgid infestations. *Canadian Journal of Forest Research* 36:1331–1341.
- Daley, M., N. Phillips, C. Pettijohn, and J. Hadley. 2007. Water use by eastern hemlock (*Tsuga canadensis*) and black birch (*Betula lenta*): implications of effects of the hemlock woolly adelgid. *Canadian Journal of Forest Research* 37:2031–2040.
- Elliott, K., and W. Swank. 2008. Long-term changes in forest composition and diversity following early logging (1919–1923) and the decline of American chestnut (*Castanea dentata*). *Plant Ecology* 197:155–172.
- Elliott, K., and J. Vose. 2010. The contribution of the Coweeta Hydrologic Laboratory to developing an understanding of long-term (1934–2008) changes in managed and unmanaged forests. *Forest Ecology and Management* 261:900–910.
- Elliott, K., J. Vose, W. Swank, and P. Bolstad. 1999. Long-term patterns in vegetation–site relationships in a southern Appalachian forest. *Journal of the Torrey Botanical Society* 126:320–334.
- Ellison, A. M., et al. 2005. Loss of foundation species: consequences for the structure and dynamics of forested ecosystems. *Frontiers in Ecology and the Environment* 9:479–486.
- Eschtruth, A., N. Cleavitt, J. Battles, R. Evans, and T. Fahey. 2006. Vegetation dynamics in declining eastern hemlock stands: 9 years of forest response to hemlock woolly adelgid infestation. *Canadian Journal of Forest Research* 36:1435–1450.
- Ford, C., K. Elliott, B. Clinton, B. Kloeppel, and J. Vose. 2012. Forest dynamics following eastern hemlock mortality in the southern Appalachians. *Oikos* 121:523–536.
- Ford, C., R. Hubbard, B. Kloeppel, and J. Vose. 2007. A comparison of sap flux-based evapotranspiration estimates



- with catchment-scale water balance. *Agricultural and Forest Meteorology* 145:176–185.
- Ford, C., R. Hubbard, and J. Vose. 2011a. Quantifying structural and physiological controls on variation in canopy transpiration among planted pine and hardwood species in the southern Appalachians. *Ecohydrology* 4:183–195.
- Ford, C., S. Laseter, W. Swank, and J. Vose. 2011b. Can forest management be used to sustain water-based ecosystem services in the face of climate change? *Ecological Applications* 21:2049–2067.
- Ford, C., and J. Vose. 2007. *Tsuga canadensis* (L.) Carr. mortality will impact hydrologic processes in southern Appalachian forest ecosystems. *Ecological Applications* 17:1156–1167.
- Gordon, D. 1998. Effects of invasive, non-indigenous plant species on ecosystem processes: lessons from Florida. *Ecological Applications* 8:975–989.
- Granier, A. 1985. Une nouvelle méthode pour la mesure du flux de sève brute dans le tronc des arbres. *Annales des Sciences Forestières* 42:193–200.
- Granier, A., and L. Loustau. 1994. Measuring and modeling the transpiration of a maritime pine canopy from sap-flow data. *Agricultural and Forest Meteorology* 71:61–81.
- Hadley, J., P. Kuzeja, M. Daley, N. Phillips, T. Mulcahy, and S. Singh. 2008. Water use and carbon exchange of red oak- and eastern hemlock-dominated forests in the north-eastern USA: implications for ecosystem level effects of hemlock woolly adelgid. *Tree Physiology* 28:15–27.
- Hall, E. 2008. Leaf-level physiological activity of *Rhododendron maximum* in response to several environmental factors. Thesis. University of Georgia, Athens, Georgia.
- Hänninen, H., and K. Tanino. 2011. Tree seasonality in a warming climate. *Trends in Plant Science* 16:412–416.
- Held, I., and B. Soden. 2006. Robust responses of the hydrologic cycle to global warming. *Journal of Climate* 19:5686–5699.
- IPCC. 2007. Contribution of Working Groups I, II, and III to the Fourth Assessment Report of the Intergovernmental Panel on Climate Change. IPCC, Geneva, Switzerland.
- Jarvis, P. 1976. The interpretation of the variations in leaf water potential and stomatal conductance found in canopies in the field. *Philosophical Transactions of the Royal Society of London* 273:593–610.
- Jonas, S., W. Xi, J. Waldron, and R. Coulson. 2012. Impacts of hemlock decline and ecological considerations for hemlock stand restoration following hemlock woolly adelgid outbreaks. *Tree and Forestry Science and Biotechnology* 6:22–26.
- Katul, G., S. Manzoni, S. Palmroth, and R. Oren. 2009. A stomatal optimization theory to describe the effects of atmospheric CO<sub>2</sub> on leaf photosynthesis and transpiration. *Annals of Botany* 105:431–442.
- Knoepp, J., J. Vose, B. Clinton, and M. Hunter. 2012. Hemlock infestation and mortality: impacts on nutrient pools and cycling in Appalachian forests. *Soil Science Society of America Journal* 75:1935–1945.
- Krapfl, K., E. Holzmüller, and M. Jenkins. 2011. Early impacts of hemlock woolly adelgid in *Tsuga canadensis* forest communities of the southern Appalachian Mountains. *Journal of the Torrey Botanical Society* 138:93–106.
- Labat, D., Y. Godderis, J. Probst, and J. Guyot. 2004. Evidence for global runoff increase related to climate warming. *Advances in Water Resources* 27:631–642.
- Landsberg, J., and R. Waring. 1997. A generalized model of forest productivity using simplified concepts of radiation-use efficiency, carbon balance and partitioning. *Forest Ecology and Management* 95:209–228.
- Laseter, S., C. Ford, J. Vose, and L. Swift. 2012. Long-term temperature and precipitation trends at the Coweeta Hydrologic Laboratory, Otto, North Carolina, USA. *Hydrologic Research* 43:890–901.
- Lei, T., S. Semones, J. Walker, B. Clinton, and E. Nilsen. 2002. Effects of *Rhododendron maximum* thickets on tree seed dispersal, seedling morphology, and survivorship. *International Journal of Plant Sciences* 163:991–1000.
- Lowe, P. 1977. An approximating polynomial for the computation of saturation vapor pressure. *Journal of Applied Meteorology* 16:100–103.
- Martin, J., B. Kloeppel, T. Schaefer, D. Kimbler, and S. McNulty. 1999. Aboveground biomass and nitrogen allocation of ten deciduous southern Appalachian tree species. *Canadian Journal of Forest Research* 28:1648–1659.
- Medlyn, B., et al. 2001. Stomatal conductance of forest species after long-term exposure to elevated CO<sub>2</sub> concentration: a synthesis. *New Phytologist* 149:247–264.
- Narayananaraj, G., P. Bolstad, K. Elliott, and J. Vose. 2009. Terrain and landform influence on *Tsuga canadensis* (L.) Carrière (eastern hemlock) distribution in the southern Appalachian Mountains. *Castanea* 75:1–18.
- Niinemets, U., I. Wright, and J. Evans. 2009. Leaf mesophyll diffusion conductance in 35 Australian sclerophylls covering a broad range of foliage structural and physiological variation. *Journal of Experimental Botany* 60:2433–2449.
- Nuckolls, A. 2007. The effects of hemlock woolly adelgid (*Adelges tsugae*) damage on short-term carbon cycling in southern Appalachian eastern hemlock (*Tsuga canadensis*) stands. Thesis. University of Georgia, Athens, Georgia, USA.
- Nuckolls, A., N. Wurzbarger, C. Ford, R. Hendrick, J. Vose, and B. Kloeppel. 2009. Hemlock declines rapidly with hemlock woolly adelgid infestation and impacts the carbon cycle in southern Appalachian forests. *Ecosystems* 12:179–190.
- Orwig, D., and D. Foster. 1998. Forest response to the introduced hemlock woolly adelgid in southern New England, USA. *Journal of the Torrey Botanical Society* 125:60–73.
- Orwig, D., J. Thompson, N. Povak, M. Manner, and D. Niebyl. 2012. A foundation tree at the precipice: *Tsuga canadensis* health after the arrival of *Adelges tsugae* in central New England. *Ecosphere* 3:art10.
- Pataki, D., S. Bush, P. Gardner, D. Solomon, and J. Ehleringer. 2005. Ecohydrology in a Colorado River riparian forest: implications for the decline of *Populus fremontii*. *Ecological Applications* 15:1009–1018.
- Peck, M., E. Russek-Cohen, D. Wait, and I. Forseth. 2002. Ecophysiological response curve analysis using nonlinear mixed models. *Oecologia* 132:175–180.
- Phillips, N., R. Oren, and R. Zimmermann. 1996. Radial patterns of xylem sap flow in non-, diffuse- and ring-porous tree species. *Plant Cell and Environment* 19:983–990.
- Pontailleur, J. 1990. A cheap quantum sensor using a gallium arsenide photodiode. *Functional Ecology* 4:591–596.
- Russell, R., T. Lei, and E. Nilsen. 2009. Freezing induced leaf movements and their potential implications to early spring carbon gain: *Rhododendron maximum* as exemplar. *Functional Ecology* 23:463–471.
- Santee, W. 1978. A dimensional analysis of eastern hemlock (*Tsuga canadensis*). Thesis. University of Georgia, Athens, Georgia, USA.
- Santee, W., and C. Monk. 1981. Stem diameter and dry weight relationships in *Tsuga canadensis* (L.) Carr. *Bulletin of the Torrey Botanical Club* 108:320–323.
- Scott, R., T. Huxman, D. Williams, and D. Goodrich. 2006. Ecohydrological impacts of woody-plant encroachment: seasonal patterns of water and carbon dioxide exchange within a semiarid riparian environment. *Global Change Biology* 12:311–324.
- Spaulding, H., and L. Rieske. 2010. The aftermath of an invasion: Structure and composition of Central Appalachian hemlock forests following establishment of the hemlock

- woolly adelgid, *Adelgis tsugae*. *Biological Invasions* 12:3135–3143.
- Swift, L., G. Cunningham, and J. Douglass. 1988. Climate and hydrology. Pages 35–55 in W. Swank and D. Crossley, editors. *Ecological Studies*. Volume 66: Forest hydrology and ecology at Coweeta. Springer-Verlag, New York, New York, USA.
- Vose, J., N. Sullivan, B. Clinton, and P. Bolstad. 1995. Vertical leaf-area distribution, light transmittance, and application of the Beer-Lambert law in four mature hardwood stands in the southern Appalachians. *Canadian Journal of Forest Research* 25:1036–1043.
- Vose, J., and W. Swank. 1994. Effects of long-term drought on the hydrology and growth of a white pine plantation in the southern Appalachians. *Forest Ecology and Management* 64:25–39.
- Walter, M., D. Wilks, J. Parlange, and R. Schneider. 2004. Increasing evapotranspiration from the conterminous United States. *Journal of Hydrometeorology* 5:405–408.
- Ward, J., and G. Stephens. 1996. Influence of crown class on survival and development of *Betula lenta* in Connecticut, USA. *Canadian Journal of Forest Research* 26:277–288.
- Warren, J., E. Potzelsberger, S. Wullschlegel, P. Thornton, H. Hasenauer, and R. Norby. 2011. Ecohydrologic impact of reduced stomatal conductance on forests exposed to elevated CO<sub>2</sub>. *Ecohydrology* 4:196–210.
- Wurzbarger, N., and R. Hendrick. 2007. Rhododendron thickets alter N cycling and soil extracellular enzyme activities in southern Appalachian hardwood forests. *Pedobiologia* 50:563–576.

#### SUPPLEMENTAL MATERIAL

##### Appendix

A figure displaying species-specific leaf area data used in the calculation of leaf-level transpiration ([Ecological Archives A023-039-A1](#)).